

# Flavoprotein Hydroxylase PgaE Catalyzes Two Consecutive Oxygen-Dependent Tailoring Reactions in Angucycline Biosynthesis

Pauli Kallio,\* Pekka Patrikainen, Jukka-Pekka Suomela, Pekka Mäntsälä, Mikko Metsä-Ketelä, and Jarmo Niemi

Department of Biochemistry and Food Chemistry, University of Turku, FIN-20014 Turku, Finland

 Supporting Information

**ABSTRACT:** A simplified model system composed of a NADPH-dependent flavoprotein hydroxylase PgaE and a short-chain alcohol dehydrogenase/reductase (SDR) CabV was used to dissect a multistep angucycline modification redox cascade into several subreactions in vitro. We demonstrate that the two enzymes are sufficient for the conversion of angucycline substrate 2,3-dehydro-UWM6 to gaudimycin C. The flavoenzyme PgaE is shown to be responsible for two consecutive NADPH- and O<sub>2</sub>-dependent reactions, consistent with the enzyme-catalyzed incorporation of oxygen atoms at C-12 and C-12b in gaudimycin C. The two reactions do not significantly overlap, and the second catalytic cycle is initiated only after the original substrate 2,3-dehydro-UWM6 is nearly depleted. This allowed us to isolate the product of the first reaction at limiting NADPH concentrations and allowed the study of the qualitative and kinetic properties of the separated reactions. Dissection of the reaction cascade also allowed us to establish that the SDR reductase CabV catalyzes the final biosynthetic step, which is closely coupled to the second PgaE reaction. In the absence of CabV, the complete PgaE reaction leads invariably to product degradation, whereas in its presence, the reaction yields the final product, gaudimycin C. The result implies that the C-6 ketoreduction step catalyzed by CabV is required for stabilization of a reactive intermediate. The close relationship between PgaE and CabV would explain previous in vivo observations: why the absence of a reductase gene may result in the lack of C-12b-oxygenated species and, vice versa, why all C-12b-oxygenated angucyclines appear to have undergone reduction at position C-6.



Angucyclines, a group of aromatic polyketide secondary metabolites assembled around a benz[*a*]anthraquinone core, are produced by various members of the bacterial genus *Streptomyces*. To date, several hundred angucycline compounds have been isolated and characterized, and many of them have been reported to have activities of potential interest, including antibacterial<sup>1–3</sup> and antitumor<sup>4,5</sup> functions. The most extensively studied biosynthetic pathways include clusters expressing landomycin (*lan*, *Streptomyces cyanogenus*), urdamycin (*urd*, *Streptomyces fradiae*), jadomycin (*jad*, *Streptomyces venezuelae*), and gaudimycins (*pga*, *Streptomyces* sp. PGA64; *cab*, *Streptomyces* sp. H021). These pathways have been characterized to varying extents in vivo and in vitro and serve as primary model systems in the elucidation of the enzyme-catalyzed biosynthetic steps behind natural product diversity.

The biosynthesis of angucyclines follows a well-defined type II aromatic polyketide pathway to form a common angucycline intermediate UWM6.<sup>6–8</sup> Our current focus is on the subsequent post-PKS tailoring reactions, which cause structural variation between the different pathways. Together with variable glycosylation patterns, alternative redox modification regimes are responsible for the functional diversity of naturally occurring angucyclines, but at present, there is no exact consensus about how each outcome is accomplished.

The angucycline modification reactions involve several successive oxygenation and reduction steps. These reactions are

catalyzed by a composite of enzymes from three enzyme families, FAD-dependent aromatic hydroxylases, flavoprotein oxygenases, and short-chain alcohol dehydrogenase/reductases (SDRs). One of the initial modification steps is the hydroxylation at position C-12. Although this reaction has been reported to take place spontaneously for UWM6 in vitro,<sup>6,8</sup> the step is usually affiliated with NADPH-dependent aromatic hydroxylases such as UrdE,<sup>9</sup> LndE,<sup>10</sup> PgaE,<sup>11</sup> JadH,<sup>12</sup> and OvmOI.<sup>5</sup> The subsequent oxidation of the hydroquinone to the C-7,12-quinone structure common to all angucycline metabolites is generally thought to occur nonenzymatically. Depending on the pathway, the C-12 hydroxylation is followed by reactions including oxygenation at position C-12b, dehydration between C-2 and C-3 atoms and C-4a and C-12b atoms, ketoreduction at position C-6, and possible aromatization of angucycline rings B and A. Enzymes reported to have a role in these catalytic events are flavoprotein oxygenases and SDR reductases found in several alternative combinations. The two enzymes may be translated as a fusion protein as exemplified by LanM2, UrdM, and PgaM, or they can be expressed as separate entities as in the case of CabV and CabM. In some cases, the SDR reductase may be completely missing as in the

**Received:** April 20, 2011

**Revised:** May 19, 2011

**Published:** May 19, 2011

jadomycin pathway or there may be an additional copy of it as in the landomycin pathway.

The modification reactions have been shown to take place in sequential cascades that may involve unstable intermediates, putative nonenzymatic steps, strict enzyme–enzyme coupling, and/or multifunctional enzymes. As a result, dissection of the biosynthetic cascades into separate catalytic steps is not always plausible, making the elucidation of exact chemical changes and the corresponding enzyme functions challenging. For example (and as of specific interest to this study), urdamycin and gaudimycin C contain hydroxyl groups at positions C-12b and C-4a as opposed to landomycin A and jadomycin in which they are missing, yet there are no clear enzyme candidates that, on the basis of sequence homology, could account for the differences.

We have previously investigated the roles of the modification enzymes PgaE and PgaM (*pga*, *Streptomyces* sp. PGA64) in vitro. Together they catalyze the formation of gaudimycin C from an angucyclinone precursor now identified as 2,3-dehydro-UWM6. PgaE<sup>13,14</sup> is a NADPH-dependent FAD flavoprotein and a member of the pHBH aromatic hydroxylase enzyme family.<sup>15</sup> It is thought to be responsible for the C-12 hydroxylation in analogy to its homologues in related angucycline pathways. PgaM is a bipartite enzyme with an N-terminal flavoprotein oxygenase and a C-terminal SDR reductase domain fused together at the translational level.<sup>16</sup> When coupled to the PgaE reaction, PgaM was shown to catalyze the subsequent steps in gaudimycin C biosynthesis. The PgaE and PgaM reaction, however, was strictly dependent on the simultaneous presence of both enzymes, and separation of the reactions led to intermediate degradation and the corresponding decrease in the level of product formation. Further attempts to dissect the catalytic reactions were unsuccessful as the N-terminal oxygenase domain of PgaM (PgaMox) expressed alone did not exhibit any catalytic activity with PgaE, and despite extensive efforts, the corresponding C-terminal SDR domain (PgaMred) could not be recovered in soluble form. From this premise, the objective of this study was to further delineate the catalytic sequence in gaudimycin C formation and directly elucidate the order and functions of the enzymatic reactions. The idea was to substitute the insoluble reductase domain PgaMred with the homologous independent SDR enzyme CabV (*cab*, *Streptomyces* sp. H021)<sup>11</sup> to separate the oxygenase and reductase activities from one another.

## MATERIALS AND METHODS

**Expression, Purification, and Analysis of the Primary Substrate.** The substrate 2,3-dehydro-UWM6 was expressed in *Streptomyces lividans* TK24/pMC6BD.<sup>7</sup> Precultures (TSB with 10  $\mu$ g/mL thiostreptone) were grown for 3–4 days at 30 °C and used to inoculate the main cultures (E1 with 20 g/L XAD-7 resin as an absorbent). Volumes of the parallel cultures were 150, 100, and 50 mL conducted in 1 L, 500 mL, and 250 mL Erlenmeyer flasks, respectively. The cultures were incubated for 7 days at 30 °C with 350 rpm shaking. The XAD with bound metabolites was isolated from the culture broth by decanting and washing with water, followed by elution with methanol. The compounds were then extracted under acidic conditions (HCl) with water and chloroform, followed by repeated washes with water until the aqueous phase was colorless. The compounds were solubilized in methanol and purified using preparative scale high-performance liquid chromatography (HPLC) (Merck Hitachi L4250 UV–vis detector, L-6200A Intelligent Pump, Merck LiChroCART 250-10

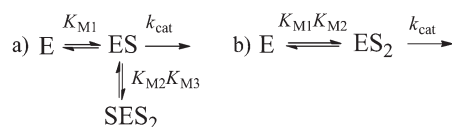
column LiChrospher 100 RP-18/10  $\mu$ M) with a gradient from 15% acetonitrile with 0.1% HCOOH to 100% acetonitrile at a flow rate 2.5 mL/min. The main peak fractions were pooled, dried, and further purified using repeated rounds of selective solubilization with methanol. The extracted product was analyzed by HPLC and liquid chromatography–mass spectroscopy (LC–MS) and confirmed as 2,3-dehydro-UWM6 via comparison with the authentic standard from *S. venezulae* VS668.<sup>12</sup> The yield of the purified substrate was typically 1–2 mg/L of culture. The working stock solution was prepared in methanol to a final concentration  $\sim$ 500  $\mu$ M.

**Construct, Expression, and Purification of CabV.** The *cabV* gene was amplified with Phusion DNA polymerase (Finnzymes) using *Streptomyces* sp. H021 chromosomal DNA as a template. The following primers were used: 5'-TATAGATCTGGAAAGCTCGCGAACAAG-3' (sense) and 5'-TATAGATCTTCAGCCGAGGAGTGTGCC-3' (antisense) (ordered from TAG Copenhagen). The amplified gene was subcloned into pBHBA<sup>17</sup> as a *Bgl*III fragment, and the orientation was confirmed by analytical digestion. The construct was verified by sequencing. CabV was expressed as an N-terminal His-tagged fusion in *Escherichia coli* strain TOP10 (2 $\times$ YT medium in 250 mL/1 L Erlenmeyer, 0.02% L-arabinose induction at an OD<sub>600</sub> of 0.5, incubation at 30 °C with 250 rpm shaking for 16 h). The cells were harvested and washed followed by lysis using a French pressure cell press (SLM Aminco). The protein was purified in a single step using a 5 mL HisTrap Ni<sup>2+</sup>-affinity column (Amersham Biosciences) and eluted according to the manufacturer's instructions with 0.5 M imidazole. Glycerol was added to a final concentration of 50% in the elution peak fractions, followed by analysis by sodium dodecyl sulfate–polyacrylamide gel electrophoresis to confirm purity. The protein concentration was estimated using the Bradford dye binding method alongside NanoOrange Protein Quantitation Kit (Invitrogen). The protein was stored at –20 °C in 25 mM Na<sub>3</sub>PO<sub>4</sub> · 12H<sub>2</sub>O, 75 mM NaCl, 125–250 mM imidazole, and 50% glycerol (pH 7.0).

**Enzyme Reactions in Vitro.** The in vitro reactions were typically conducted at room temperature in 100 mM potassium phosphate buffer (pH 7.6) containing 30–100  $\mu$ M NADPH (Sigma catalog no. N1630) and 30–35  $\mu$ M substrate supplied in methanol [in all reaction mixtures, the final methanol concentration was always 6% (v/v)]. The two alternate substrates were 2,3-dehydro-UWM6 or the corresponding PgaE/2,3-dehydro-UWM6 product [prepared fresh for each individual reaction (see below)]. The enzyme concentrations were typically 150 nM PgaE with additional 150–600 nM CabV or PgaMox in the coupled reaction mixtures. As an exception, the kinetic assays were conducted using 30 nM PgaE to ensure a sufficient number of data points within the linear area of the progress curve. The total reaction volumes ranged between 200  $\mu$ L and 1 mL depending on the application but could be scaled up to >10 mL when necessary. The reactions were initiated by the addition of PgaE, the mixtures mixed carefully with a pipet, and the reactions allowed to proceed at  $\sim$ 22 °C.

**Metabolite Extraction.** Isolation of 2,3-dehydro-UWM6 and gaudimycin C from the reaction mixtures was performed by three repeated chloroform extractions (1:4 vol chloroform per extraction) followed by desiccation and resolubilization in methanol.<sup>14</sup> Isolation of the more hydrophilic PgaE/2,3-dehydro-UWM6 product was achieved with pre-equilibrated 1 mL solid phase extraction columns (Discovery DSC-18/SUPELCO) and eluted in methanol. To obtain a maximal yield of the product,

**Scheme 1. Simplified Reaction Scheme for (a) the First Reaction of PgaE and (b) the Second Reaction of PgaE As Suggested by the Kinetic Data**



the NADPH concentration was always optimized for each new reaction series, and multiple extractions were conducted simultaneously to allow increased elution volumes and better repeatability.

**Analytical HPLC.** The reaction compounds were analyzed by RP-HPLC (Schimadzu VP series chromatography system with a diode array detector, SPD-M10Avp) using a C-18 reverse phase column (Merck LiChrospher 100 RP-18/5  $\mu$ m). The elution gradient was from 15% acetonitrile with 0.1% HCOOH to 95% acetonitrile ( $T_{tot} = 55$  min) at a flow rate of 0.5 mL/min. The substrate 2,3-dehydro-UWM6 and gaudimycin C were quantified and compared on the basis of the respective peak areas at the specific absorbance maxima of 406 and 428 nm, respectively.

**Spectrophotometric Measurements.** Consumption of 2,3-dehydro-UWM6 by PgaE was monitored spectrophotometrically at 406 nm.<sup>14</sup> Conversion of the isolated PgaE/2,3-dehydro-UWM6 product was monitored accordingly at 510 nm. The reactions were conducted in a cuvette (Shimadzu UV-1601/GE Healthcare GeneQuant 1300) or on a 96-well plate (PerkinElmer Victor<sup>3</sup> 1420 Multilabel Counter/Molecular Devices SpectraMax 384plus).

**Analysis of Kinetic Data.** The kinetic parameters for each substrate were determined from the initial slopes of declining progression curves at different substrate concentrations. All calculations were based on the presumption that substrate dilution prior to application had no effect on the relative loss (e.g., via binding to surfaces) and that the extraction yield of the PgaE/2,3-dehydro-UWM6 product was 100%. Data analysis was performed using Origin 8.0. Rate equations for the mechanisms in parts a and b of Scheme 1 are provided by eqs 1 and 2, respectively.

$$V_o = \frac{k_{cat}[E_{total}]}{1 + \frac{K_{M1}}{[S]} + \frac{[S]^2}{K_{M2}K_{M3}}} \quad (1)$$

$$V_o = \frac{k_{cat}[E_{total}]}{1 + \frac{K_{M1}K_{M2}}{[S]^2}} \quad (2)$$

**LC–MS and <sup>18</sup>O Incorporation.** MS analyses were performed with a Micromass Quattro Premier tandem quadrupole mass spectrometer (Waters Corp.) using positive ESI. The capillary voltage was set at 3 kV and the sample cone voltage at 30 V. The source and the desolvation temperatures were set at 100 and 150 °C, respectively. Nitrogen was used as the desolvation and cone gas, and the flows were set at 400 and 50 L/h, respectively. The MS analysis was preceded by LC separation of the compounds using equivalent HPLC equipment and conditions as described for analytical HPLC above.

**Fluorometric Analysis of NADPH Consumption.** Kinetic NADPH quantitation of parallel 200  $\mu$ L reaction mixtures was

conducted on a 96-well plate (PerkinElmer Victor<sup>3</sup> 1420 Multilabel Counter) or in 0.5 mL to 1 mL volumes in a cuvette (Varian Cary Eclipse fluorescence spectrophotometer) by measuring fluorescence (355 nm excitation/460 nm emission). Under the conditions tested, the substrate 2,3-dehydro-UWM6 or the product(s) formed did not have any considerable effect on the assay. The quantitation was further validated using a commercial NADP<sup>+</sup>/NADPH quantitation kit (BioVision catalog no. K347-100).

**Anaerobic Reactions and Incorporation of <sup>18</sup>O.** Anaerobic reaction conditions were achieved using a Thunberg cuvette in combination with a self-assembled airtight valve system connected to a vacuum and a nitrogen source. Aided by brief ultrasound bath treatments, this allowed efficient removal of solubilized oxygen prior to mixing of the reaction components. The system was further attached to a pressurized container of <sup>18</sup>O, which allowed the introduction of 99% <sup>18</sup>O<sub>2</sub> (Sigma-Aldrich). In the corresponding H<sub>2</sub><sup>18</sup>O reactions, 50–75% (v/v) of the reaction buffer was replaced by H<sub>2</sub><sup>18</sup>O (Sigma-Aldrich). In applications where aerobic conditions did not have to be restored, glucose oxidase/catalase treatment<sup>18</sup> was used in parallel to verify the results. The reaction was performed by a 3 min preincubation of the reaction mixture with 50 mM glucose, 0.1  $\mu$ M glucose oxidase (Fluka Analytical), and 1.5  $\mu$ M catalase (Sigma-Aldrich) prior to addition of PgaE.

## RESULTS

**Production of the 2,3-Dehydro-UWM6 Substrate for the Enzymatic Reactions.** The substrate for the in vitro assays was extracted from *S. lividans* expression strain TK24/pMC6BD<sup>7</sup> as described in Materials and Methods. Detailed analysis of the production profile revealed, unexpectedly, that the main metabolite in the isolates was 2,3-dehydro-UWM6, a dehydrated derivative of the biosynthetic intermediate UWM6 also produced by the strain (Figure S1 of the Supporting Information). The equivalent 2,3-dehydro-UWM6 elution fraction had been used as a default substrate in the earlier studies<sup>14</sup> and, although identified incorrectly at the time, was used throughout the following in vitro assays to allow direct comparison. The purified 2,3-dehydro-UWM6 was apparently stable and did not undergo nonenzymatic conversion in methanol, chloroform extraction or under the aqueous reaction conditions tested (Figure 1a).

**Expression Constructs and Enzyme Production.** The gene encoding CabV was successfully cloned into a modified pBAD/HisB expression vector<sup>17</sup> under the control of the *ara* promoter. Using this construct, CabV was expressed as an N-terminal polyhistidine-tagged fusion protein in *E. coli* strain TOP10. The enzyme was purified via single-step Ni-affinity chromatography as described in Materials and Methods. PgaE<sup>13</sup> and PgaMox<sup>16</sup> were heterologously produced and purified as described previously.

**Formation of Gaudimycin C by PgaE and CabV in Vitro.** We have previously demonstrated that incubation of PgaE with 2,3-dehydro-UWM6 resulted in the disappearance of the substrate and the formation of numerous hydrophilic degradation products when conducted to completion in the presence of sufficient NADPH and O<sub>2</sub><sup>14</sup> (Figure 1b). Under equivalent conditions, CabV alone did not exhibit any activity toward the substrate. Combining the two reactions by incubating PgaE and CabV together with 2,3-dehydro-UWM6 (and NADPH and O<sub>2</sub>) yielded a single stable main product (Figure 1c). On the basis of the RP-HPLC retention time (coelution), UV–vis spectrum,

and mass analysis by LC–MS ( $m/z$  357.3  $[M + H]^+$ ), the compound was identified, surprisingly, as gaudimycin C.<sup>14</sup> Consistent with this finding, addition of PgaMox that had previously been associated with one of the oxygenation reactions appeared to have no effect on the reaction profile or the formation of gaudimycin C.

**Separation of Consecutive PgaE-Catalyzed Reactions.** As reported previously, oxygenation of 2,3-dehydro-UWM6 by PgaE was dependent on NADPH. Parallel kinetic quantitation of 2,3-dehydro-UWM6 (Figure 2b) and NADPH (Figure 2a) revealed, surprisingly, that a total of 2 equiv of the cosubstrate was needed in the complete reaction: 1 equiv for the initial 2,3-dehydro-UWM6 conversion and another for a subsequent,

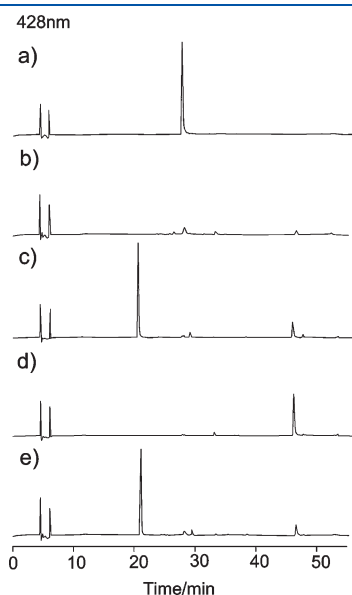


**Figure 1.** HPLC profiles ( $\lambda_{428}$ ) of complete enzymatic PgaE (and/or CabV) reactions using 2,3-dehydro-UWM6 as a substrate. (a) In the absence of the enzymes, the substrate remains unconverted. (b) Complete PgaE reaction with an excess of NADPH that results in end product degradation. (c) Coupled reaction of PgaE and CabV under equivalent conditions that yields gaudimycin C. (d) PgaE reaction conducted under limiting NADPH conditions that stalls after all substrate is consumed. A shunt derivative (dehydrorabelomycin) of the extracted product is observed via HPLC. (e) Gaudimycin C obtained if the product from the PgaE/2,3-dehydro-UWM6 reaction conducted at limiting NADPH concentrations is extracted and re-incubated with PgaE and CabV.

previously unidentified, step. On the basis of this central observation, the two reactions were separated from one another via titration of the concentration of NADPH down to approximately half of that required in total. These conditions allowed the consumption of 2,3-dehydro-UWM6 but forestalled the subsequent biosynthetic step. Consequently, the aqueous reaction mixture was left clearly red in color ( $A_{\max} = 510$  nm), consistent with the accumulation of a reaction intermediate (Figure 2c). In contrast, a reaction with an excess of NADPH continued further, resulting in the loss of the absorbance peak at 510 nm (Figure 2c) accompanied by the formation of characteristic degradation fragments.

**Recoupling of the Separated Reactions To Form Gaudimycin C.** Significantly, addition of NADPH and CabV to the incomplete PgaE reaction mixture (halted at the point where 2,3-dehydro-UWM6 had been consumed) resulted in the formation of gaudimycin C. In an analogous manner, the intermediate could be extracted using C-18 solid phase extraction (SPE) and converted further to a corresponding amount of gaudimycin C by PgaE, CabV, and NADPH (Figure 1e). Like the first reaction, these steps were dependent on the presence of  $O_2$ , and gaudimycin C was not formed if oxygen was removed after the initial PgaE/2,3-dehydro-UWM6 reaction. It is also important to notice that CabV alone was not sufficient to convert the isolated intermediate to gaudimycin C as both CabV and PgaE with NADPH were required simultaneously to complete the reaction sequence. Incubation with the enzymes CabV and PgaMox under equivalent conditions did not result in substrate turnover.

**Characterization of the Product of the First PgaE Reaction.** The PgaE/2,3-dehydro-UWM6 product was relatively unstable and degraded in a matter of minutes or hours in the aqueous reaction buffer or in methanol eluted from SPE. The observed bathochromic shift toward the red area of the visible spectrum and a clear increase in hydrophilicity were in agreement with the C-12 hydroxylation reaction proposed for the initial PgaE-catalyzed reaction.<sup>14</sup> In RP-HPLC and LC–MS analysis conducted for further confirmation, however, the compound remained undetected. The only peak relative in size was a shunt derivative ( $A_{\max} = 459$  nm), which eluted at the very hydrophobic end of the HPLC gradient (Figure 1d) and, after re-isolation, could not be further converted by PgaE (and/or CabV). Comparative HPLC analysis confirmed the eluted product as dehydrorabelomycin<sup>12</sup> formed spontaneously during the analytical procedure (data not shown).

**Analysis of the Coupled Reaction of PgaE and CabV.** The NADPH consumption pattern was further examined in a coupled

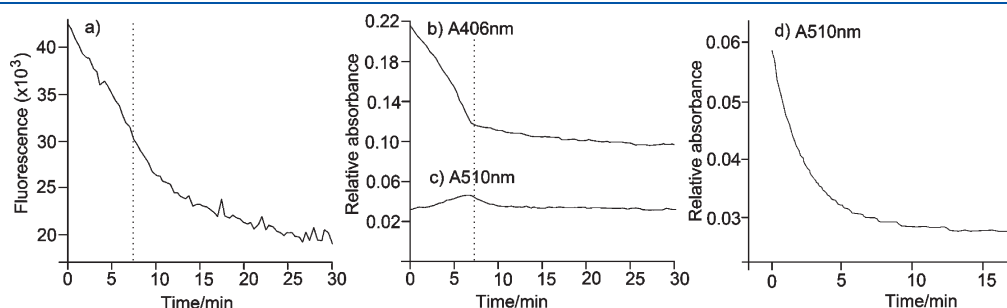


**Figure 2.** Fluorometric and spectrophotometric comparison of the two PgaE-catalyzed reactions. Simultaneous consumption of (a) NADPH and (b) 2,3-dehydro-UWM6 in a complete PgaE reaction (plotted on the same relative scale). (c) Parallel accumulation and disappearance of the PgaE/2,3-dehydro-UWM6 reaction product. The dashed line indicates the point of 2,3-dehydro-UWM6 depletion. (d) Reaction corresponding to trace c using the PgaE/2,3-dehydro-UWM6 product isolated with C-18 solid phase extraction as a substrate.

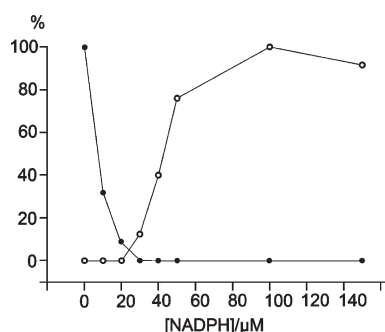


**Figure 3.** Consumption of 2,3-dehydro-UWM6 (●) and formation of gaudimycin C (○) by PgaE (and/or CabV) at different NADPH concentrations. The reactions were conducted to completion with 0–150  $\mu\text{M}$  NADPH using 30  $\mu\text{M}$  2,3-dehydro-UWM6 as a substrate, followed by quantitative extraction and analysis. The relative yields were calculated from the HPLC peak areas.

reaction of PgaE and CabV conducted with different concentrations of the cosubstrate (Figure 3). In agreement with the perceived stoichiometry (Figure 2), the results clearly indicate that 1 equiv of the cosubstrate was sufficient for the initial conversion step of 2,3-dehydro-UWM6 by PgaE. Despite the presence of CabV, gaudimycin C was not formed under these conditions. Instead, an additional supply of NADPH was required to obtain the product; the maximal yield of gaudimycin C was reached at the range of 2 equiv of NADPH with respect to 2,3-dehydro-UWM6 converted (Figure 3). Importantly, time scale analysis of the reaction by HPLC confirmed that the consumption of the substrate and the formation of the final product did not significantly overlap. Most 2,3-dehydro-UWM6 was converted before any gaudimycin C was observed (Figure 4). To examine whether this was directly due to the involvement of substrate-level inhibition between the two successive PgaE-catalyzed steps, we reapplied 2,3-dehydro-UWM6 to the reaction mixture shortly before the initial supply ran out. As a result, the sequential reactions were delayed, and gaudimycin C was not detected until after the second substrate batch had also been consumed. The final yield of gaudimycin C increased accordingly and was proportional to the amount of 2,3-dehydro-UWM6 supplied in total (Figure S2 of the Supporting Information).

**Kinetics of the First and Second PgaE Reaction.** Kinetic parameters for the two individual PgaE-catalyzed reactions were measured separately using 2,3-dehydro-UWM6 and the corresponding isolated PgaE/2,3-dehydro-UWM6 product as substrates. In each case, the initial rate of substrate consumption was determined spectrophotometrically at the respective absorption maximum [406 or 510 nm (see Figure 2b,d)] and plotted versus concentration (Figure 5). The foremost observation was that the conversion of 2,3-dehydro-UWM6 by PgaE did not conform to classical Michaelis–Menten saturation kinetics but followed a profile typical of substrate inhibition. The initial reaction velocity first increased in a hyperbolic manner in relation to  $[S]$ , but instead of reaching a characteristic saturation plateau at  $V_{\text{max}}$ , the reaction rate declined at higher concentrations (Figure 5a). The highest observed initial rate of  $1.8 \pm 0.1 \text{ s}^{-1}$  was measured under the default conditions [100 mM potassium phosphate buffer (pH 7.6) and 6% (v/v) methanol] at 8.2  $\mu\text{M}$  substrate. As the profile represents a superimposition of the ascending curve and the counteracting inhibitory curve, it could not be directly used to derive the standard Michaelis constants  $k_{\text{cat}}$  and  $K_{\text{M}}$ . A simplified

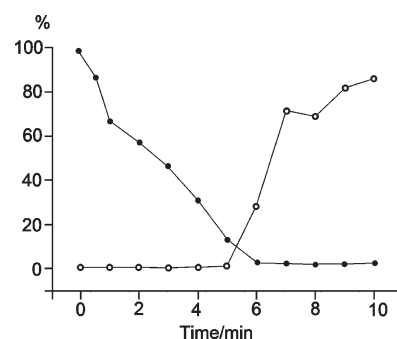


**Figure 4.** Simultaneous quantitative HPLC analysis of 2,3-dehydro-UWM6 (●) and gaudimycin C (○) in a coupled reaction of PgaE and CabV with an excess of NADPH. The samples were extracted and analyzed at 1 min intervals until the reaction has proceeded to completion (10 min). The relative yields were calculated from quantitative analytical HPLC peak areas.

allosteric inhibitory model (eq 1 in Materials and Methods) was found to adequately describe the data and used to obtain the fit in Figure 5a. Estimated from the curve fit, the independent values of  $k_{\text{cat}}$  and  $K_{\text{M}}$  for the first PgaE reaction were  $6.66 \pm 1.8 \text{ s}^{-1}$  and  $16.5 \pm 5.9 \mu\text{M}$ , respectively. Although the data for the second PgaE-catalyzed reaction could roughly be fitted using a standard hyperbolic equation, it appeared to be more appropriately described using a sigmoidal relationship (Figure 5b) (eq 2 in Materials and Methods). Within the applicable substrate concentration range (up to 140  $\mu\text{M}$ ), substrate inhibition for the second reaction was not observed. Using a freshly purified enzyme batch, the  $k_{\text{cat}}$  for the reaction was determined to be  $7.37 \pm 0.17 \text{ s}^{-1}$ . The substrate concentration at which the reaction velocity was half of the maximum was estimated to be  $18.8 \pm 0.95 \mu\text{M}$  (Materials and Methods).

**Incorporation of Oxygen from  $^{18}\text{O}_2$  and  $\text{H}_2^{18}\text{O}$ .** The fate of the oxygen atoms involved in successive PgaE reactions was studied by  $^{18}\text{O}$  isotope incorporation analysis using LC–MS. Coupled reactions of PgaE and CabV conducted under a rigorous  $^{18}\text{O}_2$  atmosphere resulted in the disappearance of the typical high-molecular mass fragmentation products of gaudimycin C, accompanied by the appearance of 2 and 4 Da ion peaks (Figure S3 of the Supporting Information). The relative abundance of the 4 Da fragments was clearly dependent on the reaction conditions and varied from almost negligible to up to two-thirds in comparison to 2 Da species in the most stringently optimized reactions. Reference reactions conducted in  $\text{H}_2^{18}\text{O}$  (under a normal atmosphere) also resulted in proportional splitting of all the major peaks into 2 Da species, but this was further shown to be caused by spontaneous exchange with water-derived oxygens. When isolated gaudimycin C produced in the absence of  $^{18}\text{O}$  was incubated with  $\text{H}_2^{18}\text{O}$ , the characteristic 2 and 4 Da peaks became visible within the time frame used for the reactions.

## DISCUSSION

The modification reactions of angucycline antibiotics typically involve combinations of interlinked oxygenation, reduction, and dehydration steps. On the basis of the number of chemical changes and the number of putative active sites involved, these reaction cascades have been associated with multifunctional enzymes and spontaneous conversion steps in various contexts.<sup>12,14,19,20</sup> In this

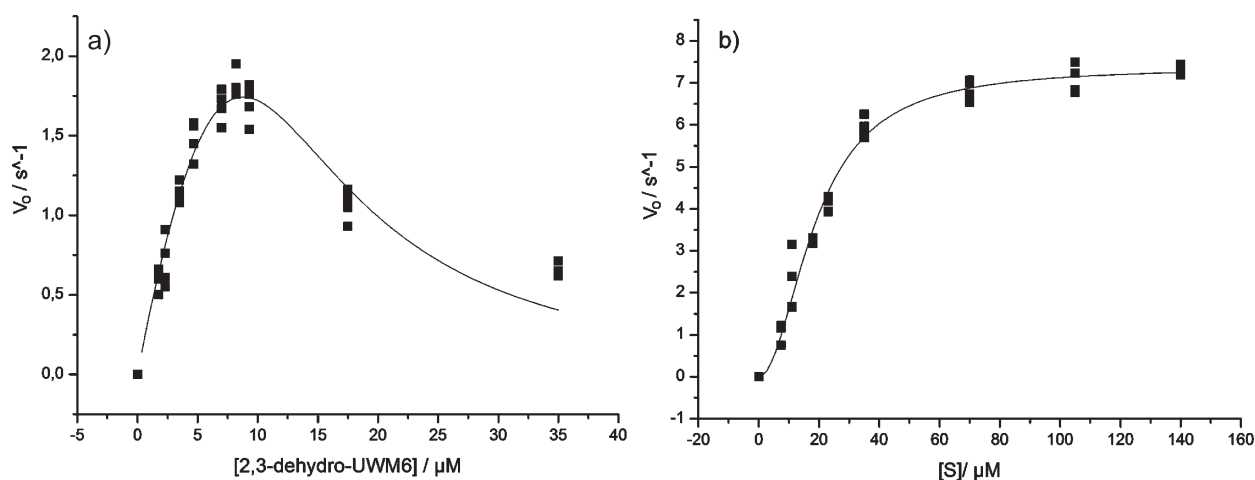
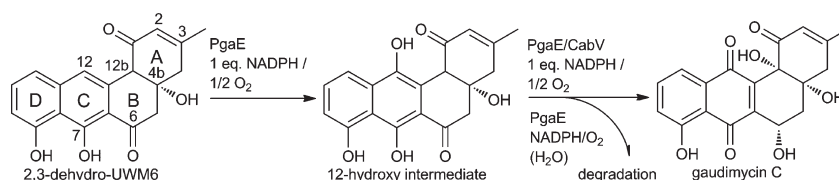


**Figure 5.** Initial reaction velocity as a function of substrate concentration for the (a) first PgaE reaction using 2,3-dehydro-UWM6 as a substrate and (b) second PgaE reaction using the C-18 solid phase-extracted product of panel a as a substrate. The reactions were conducted in an excess of NADPH and monitored spectrophotometrically at 406 and 510 nm, respectively.

**Scheme 2. Proposed Reaction Scheme for the Coupled Reaction of PgaE and CabV in Vitro Using 2,3-Dehydro-UWM6 as a Substrate in the Presence of NADPH and O<sub>2</sub><sup>a</sup>**



<sup>a</sup> The substrate carbons discussed in the context of this work are labeled. PgaE catalyzes two successive NADPH- and O<sub>2</sub>-dependent hydroxylations, and CabV reduces the carbonyl group at position 6. If the last step with PgaE and CabV is decoupled, the reaction leads to intermediate breakdown. The 7,12-quinone formation is expected to take place spontaneously.

study, we have established that PgaE (flavoprotein hydroxylase) and CabV (SDR-reductase) are able to convert the angucycline intermediate 2,3-dehydro-UWM6 to gaudimycin C in vitro when incubated in the presence of NADPH and molecular oxygen (Scheme 2). This demonstrated that the two enzymes alone were sufficient to bring about four distinct chemical changes: 12-hydroxylation, 7,12-quinone formation, 12b-hydroxylation, and 6-ketoreduction. Together with the reassessment of the structure of the substrate, the results confirmed that the single-domain SDR CabV can substitute for the two-domain oxygenase-SDR reductase PgaM in the enzymatic synthesis of gaudimycin C.<sup>16</sup>

PgaE participates in two consecutive catalytic steps as demonstrated by the isolation of the reactions from one another in vitro (Scheme 2). Our results show that first (i) PgaE converts the substrate 2,3-dehydro-UWM6 in a reaction that requires molecular oxygen and NADPH. The primary reaction product, presumably a 12-hydroxylated intermediate, is then released from the enzyme active site into the surrounding solvent. After most of the substrate 2,3-dehydro-UWM6 has been consumed, (ii) the intermediate is reassociated with PgaE for yet another cycle of catalysis which is also dependent on O<sub>2</sub> and NADPH. The observed substrate release and rebinding is necessary for the successive reactions to take place, and is consistent with the expected mechanism of FAD-dependent hydroxylases in the pHBH family. Each catalytic cycle must proceed through FAD reduction by NAD(P)H involving enzyme conformational change coupled to product dissociation.<sup>15</sup> This finding is of specific

interest as the equivalent enzymes homologous to PgaE such as CabE, LanE, and UrdE have previously been reported to participate in only a single oxygenation event in the related biosynthetic pathways.

The <sup>18</sup>O incorporation data were consistent with the association of two oxygen atoms from molecular oxygen in gaudimycin C. Earlier observations in which one of the two oxygens in the reaction of PgaE and PgaM appeared to derive from H<sub>2</sub>O and not air<sup>14</sup> could be explained by the efficient spontaneous oxygen exchange of gaudimycin C with the surrounding water.

As we have shown, the PgaE catalytic strategy involves the simultaneous presence of two alternative substrates competing for the same active site. At the same time, inspection of the PgaE crystal structure reveals that the active site cavity is large enough to accommodate the two substrate candidates in different orientations that could allow the successive reactions to take place at different positions on the substrate carbon frame.<sup>13</sup> To explicate the apparent strong preference for the initial substrate 2,3-dehydro-UWM6, the two reactions were separated from one another and independently studied with respect to their kinetic behavior in vitro. Estimated from the kinetic data, the calculated  $k_{\text{cat}}/K_M$  ratios for the first and second reactions are on the same order of magnitude, suggesting that under saturating substrate concentrations the turnover rates of the two reactions are in approximately the same range. In addition, when the two reactions are allowed to proceed one after another under the default conditions, the detected rate of the second reaction is comparable

to that of the first reaction despite the subsaturating  $[S]$ . These findings argue that the affinity difference between the two substrates alone is not sufficient to comprehensively account for the separation of the two catalytic steps.

Kinetic characterization also showed that the PgaE/2,3-dehydro-UWM6 reaction is modulated by substrate inhibition, which is a direct indication of the presence of two interacting substrate binding sites. We suspect that these sites may correspond to the alternative binding modes (or orientations) specific for the two competing substrates. Assuming the sites overlap, binding of 2,3-dehydro-UWM6 in the incorrect unproductive orientation would result in competitive inhibition of the latter catalytic cycle. Consequently, this would promote the dissociation of the two reactions into subsequent phases more efficiently than the  $K_M$  values for the individual reactions alone would suggest.

Further emphasizing the complexity of the system, the collected kinetic data suggest that the reaction may also be affected by allosteric interactions. The inhibition appears to involve cross talk between two inhibitory sites (cooperative inhibition) as first-order kinetics fail to adequately describe the relationship of  $V/[S]$  (eq 1). At the same time, the sigmoidal shape of the ascending saturation curve in Figure 5b indicates that the second reaction step may be allosterically activated by the substrate. These possibly related effects could be explained as cooperative interactions of individual PgaE subunits in the native dimer structure,<sup>13</sup> but further physical evidence is required to confirm the underlying mechanisms.

The results show that the second reaction catalyzed by PgaE results in a highly unstable product that (in the absence of CabV) is rapidly degraded in the aqueous surroundings. The degradation products are highly hydrophilic and low in molecular mass, with UV-vis properties consistent with the breakdown of the angucycline ring frame. The observed reaction resembles the oxidative reactions catalyzed by various enzymes in the breakdown of aromatic compounds such as homovanillate<sup>21</sup> or 2-methyl-3-hydroxypyridine-5-carboxylic acid (MHPC).<sup>22,23</sup> Analogous controlled oxidative ring cleavage reactions are also part of several related aromatic polyketide modification cascades and are responsible for extensive rearrangements in the carbon ring frames produced. Enzymes known to be involved in such modification reactions include MtmOIV<sup>24–26</sup> and CmmOIV<sup>27,28</sup> that catalyze the oxidative scission of the fourth ring in aureolic acid biosynthesis, JadF and JadH that together participate in jadomycin heterocycle formation<sup>29</sup> and GrhO6 that is responsible for the formation of the spiroketal moiety in griseorhodin A.<sup>30</sup>

Our results demonstrate that the outcome of the second PgaE-catalyzed reaction is stringently determined by the subsequent enzyme CabV. In the absence of CabV, the reaction leads to immediate degradation, but in its presence, the product of the second PgaE catalytic cycle is converted to gaudimycin C. Together with the fact that CabV does not have apparent activity toward the first PgaE product, this suggests that the reaction sequence in gaudimycin C biosynthesis is PgaE, PgaE, CabV, in which the last two enzymatic steps cannot be separated from one another. Although it is clear that CabV is required to stabilize the reactive intermediate and to funnel the reaction toward gaudimycin C, the exact function of the enzyme has not been demonstrated. On the basis of sequence homology, CabV is a member of the classical SDR enzyme family, members of which typically participate in redox conversions between alcohols and ketones.<sup>31–33</sup> These reactions are analogous to the C-6 carbonyl

group reduction required for gaudimycin C formation observed in our model system. Supporting this function, CabV homologues LanV and the C-terminal SDR domain of UrdM have been previously assigned for a corresponding C-6 ketoreductase activity in landomycin and urdamycin biosynthesis, respectively.<sup>19</sup> However, we have no evidence that CabV would consume NADPH as expected for the typical members of the SDR family.<sup>34–37</sup> The CabV reaction could not be isolated and directly assayed for NADPH dependence as the activity could be detected only together with PgaE, but there is no apparent difference in the amount of NADPH used in the presence and absence of CabV. These results could suggest that the reducing power in the CabV reaction does not derive directly from NADPH. As the substrate for CabV is highly oxygenated and unstable (with a putative hydroquinone structure expected to oxidize to a corresponding quinone very easily), the possibility that CabV could indirectly use the reducing power of the intermediate to conduct the C-6 ketoreduction cannot be entirely excluded.

There has been certain ambiguity about which enzyme per se is responsible for the C-12b-OH incorporation in different angucycline precursors. The two-domain flavoprotein oxygenase–SDR fusion enzymes UrdM<sup>9,38</sup> and PgaM<sup>11,14</sup> have been previously affiliated with this function in the biosynthesis of urdamycin and gaudimycins, respectively. Molecular genetic studies have shown that in the absence of *pgaM* and *urdM* C-12b-hydroxylated metabolites are not observed, which strongly suggested the involvement of the N-terminal oxygenase domains in oxygen incorporation. In the in vitro system presented here, however, the oxygenase domain PgaMox was shown to be redundant for the reaction. Instead, the absolute requirement for CabV argues that, paradoxically, it would be the C-terminal SDR domain that is needed to obtain the C-12b-hydroxylated product. The findings support the idea of mechanistic coupling between the 12b-hydroxylation and 6-ketoreduction;<sup>14</sup> the C-12b-hydroxylated angucyclines always appears to have been reduced at C-6, which could be a prerequisite for the chemical stability of these specific products. The results also underline the inadequacy of end product analysis and homology-based functional assignment alone as tools for predicting enzyme functions in these complex oxygenation cascades.

## ■ ASSOCIATED CONTENT

**S Supporting Information.** HPLC and LC–MS analysis of *Streptomyces* TK24/pMC6BD expression profile, HPLC data demonstrating competitive inhibition of the second PgaE reaction by the primary substrate 2,3-dehydro-UWM6, and LC–MS profiles showing heavy oxygen incorporation in gaudimycin C under different conditions. This material is available free of charge via the Internet at <http://pubs.acs.org>.

## ■ AUTHOR INFORMATION

### Corresponding Author

\*E-mail: [pataka@utu.fi](mailto:pataka@utu.fi). Phone: +358 23336846. Fax: +358 22317666.

### Funding Sources

This work was supported by the Academy of Finland (Grants 121688 to J.N., 127844 to P.M., and 136060 to M.M.-K.).

## ACKNOWLEDGMENT

We thank the following people for their contribution: Minna Ylihärtilä, Terhi Oja, and Kirsi Gröndahl for the CabV plasmid construct and the primary expression and purification trials; Georgi Belogurov and Anssi Malinen for valuable assistance with the interpretation of enzyme kinetic data; and Professor Keqian Yang's research group (Keqiang Fan and Xiaojing Peng) for the comparative verification of the substrate 2,3-dehydro-UWM6 and dehydrorabelomycin with their authentic standards.

## REFERENCES

- (1) Antal, N., Fiedler, H. P., Stackebrandt, E., Beil, W., Stroch, K., and Zeeck, A. (2005) Retymicin, galtamycin B, saquayamycin Z and ribofuranosyllumichrome, novel secondary metabolites from *Micromonospora* sp. Tu 6368. I. Taxonomy, fermentation, isolation and biological activities. *J. Antibiot.* 58, 95–102.
- (2) Jakeman, D. L., Bandi, S., Graham, C. L., Reid, T. R., Wentzell, J. R., and Douglas, S. E. (2009) Antimicrobial activities of jadomycin B and structurally related analogues. *Antimicrob. Agents Chemother.* 53, 1245–1247.
- (3) Abdelfattah, M., Maskey, R. P., Asolkar, R. N., Grun-Wollny, I., and Laatsch, H. (2003) Seitomycin: Isolation, structure elucidation and biological activity of a new angucycline antibiotic from a terrestrial streptomycete. *J. Antibiot.* 56, 539–542.
- (4) Korynevskaya, A., Heffeter, P., Matselyukh, B., Elbling, L., Micksche, M., Stoika, R., and Berger, W. (2007) Mechanisms underlying the anticancer activities of the angucycline landomycin E. *Biochem. Pharmacol.* 74, 1713–1726.
- (5) Lombo, F., Abdelfattah, M. S., Brana, A. F., Salas, J. A., Rohr, J., and Mendez, C. (2009) Elucidation of oxygenation steps during oviedomycin biosynthesis and generation of derivatives with increased antitumor activity. *ChemBioChem* 10, 296–303.
- (6) Kulowski, K., Wendt-Pienkowski, E., Han, L., Yang, K., Vining, L. C., and Hutchinson, C. R. (1999) Functional Characterization of the *jadI* Gene As a Cyclase Forming Angucyclinones. *J. Am. Chem. Soc.* 121, 1786–1794.
- (7) Metsä-Ketelä, M., Palmu, K., Kunnari, T., Ylihönko, K., and Mäntälä, P. (2003) Engineering anthracycline biosynthesis toward angucyclines. *Antimicrob. Agents Chemother.* 47, 1291–1296.
- (8) Kharel, M. K., Pahari, P., Lian, H., and Rohr, J. (2010) Enzymatic total synthesis of rabelomycin, an angucycline group antibiotic. *Org. Lett.* 12, 2814–2817.
- (9) Faust, B., Hoffmeister, D., Weitnauer, G., Westrich, L., Haag, S., Schneider, P., Decker, H., Kunzel, E., Rohr, J., and Bechthold, A. (2000) Two new tailoring enzymes, a glycosyltransferase and an oxygenase, involved in biosynthesis of the angucycline antibiotic urdamycin A in *Streptomyces fradiae* Tu2717. *Microbiology* 146 (Part 1), 147–154.
- (10) Baig, I., Kharel, M., Kobylansky, A., Zhu, L., Rebets, Y., Ostash, B., Luzhetskyy, A., Bechthold, A., Fedorenko, V. A., and Rohr, J. (2006) On the acceptor substrate of C-glycosyltransferase UrdGT2: Three prejadomycin C-Glycosides from an engineered mutant of *Streptomyces globisporus* 1912  $\Delta$ IndE(urdGT2). *Angew. Chem., Int. Ed.* 45, 7842–7846.
- (11) Palmu, K., Ishida, K., Mäntälä, P., Hertweck, C., and Metsä-Ketelä, M. (2007) Artificial reconstruction of two cryptic angucycline antibiotic biosynthetic pathways. *ChemBioChem* 8, 1577–1584.
- (12) Chen, Y. H., Wang, C. C., Greenwell, L., Rix, U., Hoffmeister, D., Vining, L. C., Rohr, J., and Yang, K. Q. (2005) Functional analyses of oxygenases in jadomycin biosynthesis and identification of JadH as a bifunctional oxygenase/dehydrase. *J. Biol. Chem.* 280, 22508–22514.
- (13) Koskineniemi, H., Metsä-Ketelä, M., Dobritzsch, D., Kallio, P., Korhonen, H., Mäntälä, P., Schneider, G., and Niemi, J. (2007) Crystal structures of two aromatic hydroxylases involved in the early tailoring steps of angucycline biosynthesis. *J. Mol. Biol.* 372, 633–648.
- (14) Kallio, P., Liu, Z., Mäntälä, P., Niemi, J., and Metsä-Ketelä, M. (2008) Sequential action of two flavoenzymes, PgaE and PgaM, in

angucycline biosynthesis: Chemoenzymatic synthesis of gaudimycin C. *Chem. Biol.* 15, 157–166.

- (15) Entsch, B., and van Berkel, W. J. (1995) Structure and mechanism of para-hydroxybenzoate hydroxylase. *FASEB J.* 9, 476–483.
- (16) Kallio, P., Liu, Z., Mäntälä, P., Niemi, J., and Metsä-Ketelä, M. (2007) A nested gene in *Streptomyces bacteria* encodes a protein involved in quaternary complex formation. *J. Mol. Biol.* 375, 1212–1221.
- (17) Kallio, P., Sultana, A., Niemi, J., Mäntälä, P., and Schneider, G. (2006) Crystal structure of the polyketide cyclase AknH with bound substrate and product analogue: Implications for catalytic mechanism and product stereoselectivity. *J. Mol. Biol.* 357, 210–220.
- (18) Fabian, J. (1965) Simple Method of Anaerobic Cultivation, with Removal of Oxygen by a Buffered Glucose Oxidase-Catalase System. *J. Bacteriol.* 89, 921.
- (19) Mayer, A., Taguchi, T., Linnenbrink, A., Hofmann, C., Luzhetskyy, A., and Bechthold, A. (2005) LanV, a bifunctional enzyme: Aromatase and ketoreductase during landomycin A biosynthesis. *ChemBioChem* 6, 2312–2315.
- (20) Zhu, L., Ostash, B., Rix, U., Nur-E-Alam, M., Mayers, A., Luzhetskyy, A., Mendez, C., Salas, J. A., Bechthold, A., Fedorenko, V., and Rohr, J. (2005) Identification of the function of gene *lndM2* encoding a bifunctional oxygenase-reductase involved in the biosynthesis of the antitumor antibiotic landomycin E by *Streptomyces globisporus* 1912 supports the originally assigned structure for landomycinone. *J. Org. Chem.* 70, 631–638.
- (21) Allison, N., Turner, J. E., and Wait, R. (1995) Degradation of homovanillate by a strain of *Variovorax paradoxus* via ring hydroxylation. *FEMS Microbiol. Lett.* 134, 213–219.
- (22) Tian, B., Tu, Y., Strid, A., and Eriksson, L. A. (2010) Hydroxylation and ring-opening mechanism of an unusual flavoprotein monooxygenase, 2-methyl-3-hydroxypyridine-5-carboxylic acid oxygenase: A theoretical study. *Chemistry* 16, 2557–2566.
- (23) Chaiyen, P., Brissette, P., Ballou, D. P., and Massey, V. (1997) Unusual mechanism of oxygen atom transfer and product rearrangement in the catalytic reaction of 2-methyl-3-hydroxypyridine-5-carboxylic acid oxygenase. *Biochemistry* 36, 8060–8070.
- (24) Rodriguez, D., Quiros, L. M., Brana, A. F., and Salas, J. A. (2003) Purification and characterization of a monooxygenase involved in the biosynthetic pathway of the antitumor drug mithramycin. *J. Bacteriol.* 185, 3962–3965.
- (25) Gibson, M., Nur-e-alam, M., Lipata, F., Oliveira, M. A., and Rohr, J. (2005) Characterization of kinetics and products of the Baeyer-Villiger oxygenase MtmOIV, the key enzyme of the biosynthetic pathway toward the natural product anticancer drug mithramycin from *Streptomyces argillaceus*. *J. Am. Chem. Soc.* 127, 17594–17595.
- (26) Beam, M. P., Bosserman, M. A., Noinaj, N., Wehenkel, M., and Rohr, J. (2009) Crystal structure of Baeyer-Villiger monooxygenase MtmOIV, the key enzyme of the mithramycin biosynthetic pathway. *Biochemistry* 48, 4476–4487.
- (27) Menendez, N., Nur-e-Alam, M., Brana, A. F., Rohr, J., Salas, J. A., and Mendez, C. (2004) Biosynthesis of the antitumor chromomycin A3 in *Streptomyces griseus*: Analysis of the gene cluster and rational design of novel chromomycin analogs. *Chem. Biol.* 11, 21–32.
- (28) Bosserman, M. A., Flórez, A. B., Shaaban, K. A., Braña, A. F., Salas, J. A., Méndez, C., and Rohr, J. (2011) Characterization of the Terminal Activation Step Catalyzed by Oxygenase CmmOIV of the Chromomycin Biosynthetic Pathway from *Streptomyces griseus*. *Biochemistry* 50, 1421–1428.
- (29) Rix, U., Wang, C., Chen, Y., Lipata, F. M., Remsing Rix, L. L., Greenwell, L. M., Vining, L. C., Yang, K., and Rohr, J. (2005) The oxidative ring cleavage in jadomycin biosynthesis: A multistep oxygenation cascade in a biosynthetic black box. *ChemBioChem* 6, 838–845.
- (30) Yunt, Z., Reinhardt, K., Li, A., Engeser, M., Dahse, H. M., Gutschow, M., Bruhn, T., Bringmann, G., and Piel, J. (2009) Cleavage of four carbon-carbon bonds during biosynthesis of the griseorhodin a spiroketal pharmacophore. *J. Am. Chem. Soc.* 131, 2297–2305.
- (31) Kavanagh, K. L., Jorvall, H., Persson, B., and Oppermann, U. (2008) Medium- and short-chain dehydrogenase/reductase gene and

protein families: The SDR superfamily: Functional and structural diversity within a family of metabolic and regulatory enzymes. *Cell. Mol. Life Sci.* 65, 3895–3906.

(32) Persson, B., Kallberg, Y., Bray, J. E., Bruford, E., Dellaporta, S. L., Favia, A. D., Duarte, R. G., Jornvall, H., Kavanagh, K. L., Kedishvili, N., Kisiela, M., Maser, E., Mindnich, R., Orchard, S., Penning, T. M., Thornton, J. M., Adamski, J., and Oppermann, U. (2009) The SDR (short-chain dehydrogenase/reductase and related enzymes) nomenclature initiative. *Chem.-Biol. Interact.* 178, 94–98.

(33) Persson, B., Kallberg, Y., Oppermann, U., and Jornvall, H. (2003) Coenzyme-based functional assignments of short-chain dehydrogenases/reductases (SDRs). *Chem.-Biol. Interact.* 143–144, 271–278.

(34) Nakajima, K., Yamashita, A., Akama, H., Nakatsu, T., Kato, H., Hashimoto, T., Oda, J., and Yamada, Y. (1998) Crystal structures of two tropinone reductases: Different reaction stereospecificities in the same protein fold. *Proc. Natl. Acad. Sci. U.S.A.* 95, 4876–4881.

(35) Benach, J., Filling, C., Oppermann, U. C., Roversi, P., Bricogne, G., Berndt, K. D., Jornvall, H., and Ladenstein, R. (2002) Structure of bacterial 3 $\beta$ /17 $\beta$ -hydroxysteroid dehydrogenase at 1.2 Å resolution: A model for multiple steroid recognition. *Biochemistry* 41, 14659–14668.

(36) Filling, C., Berndt, K. D., Benach, J., Knapp, S., Prozorovski, T., Nordling, E., Ladenstein, R., Jornvall, H., and Oppermann, U. (2002) Critical residues for structure and catalysis in short-chain dehydrogenases/reductases. *J. Biol. Chem.* 277, 25677–25684.

(37) Filling, C., Nordling, E., Benach, J., Berndt, K. D., Ladenstein, R., Jornvall, H., and Oppermann, U. (2001) Structural role of conserved Asn179 in the short-chain dehydrogenase/reductase scaffold. *Biochem. Biophys. Res. Commun.* 289, 712–717.

(38) Rix, U., Remsing, L. L., Hoffmeister, D., Bechthold, A., and Rohr, J. (2003) Urdamycin L: A novel metabolic shunt product that provides evidence for the role of the urdM gene in the urdamycin A biosynthetic pathway of *Streptomyces fradiae* TU 2717. *ChemBioChem* 4, 109–111.